

Creation of a metallic channel at the Sn/InAs(111)B surface studied using synchrotron-radiation photoelectron spectroscopy

K. Szamota-Leandersson,^{1,*} M. Göthelid,¹ J. Kanski,² L. Ilver,² G. Le Lay,³ and U. O. Karlsson¹

¹*Materials Physics, Kungliga Tekniska Högskolan, P.O. Box Electrum 229, 16440 Kista, Sweden*

²*Department of Physics, Chalmers University of Technology, S-412 96 Göteborg, Sweden*

³*CRMCN-CNRS, Campus de Luminy, case 913, F-13288 Marseille, Cedex 9, France*

(Received 21 July 2006; published 3 November 2006)

The properties of a Sn-induced two-dimensional electron gas at the As-terminated InAs(111)B(1×1) surface was studied by synchrotron radiation photoelectron spectroscopy. The two-dimensional electron gas reveals itself via a narrow structure at the Fermi level, visible close to normal emission for tin coverage in the range 0.5 to 2 monolayers. Although this electron gas exhibits properties that in several respects resemble those of intrinsic charge accumulation layers on free InAs surfaces, our observations suggest that the present electron gas is much more linked to the Sn adlayer.

DOI: [10.1103/PhysRevB.74.205406](https://doi.org/10.1103/PhysRevB.74.205406)

PACS number(s): 79.60-i, 73.21-b, 68.43-h

It is well known that a two-dimensional electron gas (2DEG) exists at InAs surfaces. Much attention has been paid to different orientations and reconstructions on clean surfaces.^{1,2} In the most studied case, InAs(110), the 2DEG is not present on the clean well-cleaved surface while it has been shown that deposition of tiny amounts (~ 0.05 ML) of Cs induce a giant band bending at the surface creating a 2DEG (Ref. 3).

The As-terminated InAs(111)B(1×1) surface belongs to an extraordinary group of polar semiconductor surfaces (including the corresponding InP and GaP ones) that are not reconstructed while other surfaces exhibit different reconstructions depending on the surface composition.⁴ In disagreement with the electron counting rule, this bulk truncated InAs(111)B(1×1) surface is stable. The stability of this surface cannot be explained by the introduction of gap states, which would accommodate a sufficient amount of charge to remove the divergent electrostatic potential. Indeed, a study by Mankefors *et al.* using *ab initio* calculations shows that the surface stability is driven by a redistribution of charge over several atomic layers, so that charge is being transferred from the surface toward the bulk.⁵ In an earlier study, we successfully used this model to describe the formation of an oxide on this InAs(111)B(1×1) surface.⁶

The electronic structure of the clean InAs(111)B(1×1) surface corresponds to flat band conditions and previous studies have shown the existence of two surface states.⁷ At variance with the reconstructed InAs(111)A(2×2) surface, this surface does not accommodate an electron accumulation layer,¹ i.e., there is no 2DEG. The creation of a 2DEG at the interface of a nonpolar-polar system, by condensing metal atoms forming α -Sn-like films on InSb has been reported.⁸ Most information available on the behavior of Sn deposited the III-V semiconductors concern studies on InSb(111)A and InSb(111)B surfaces.^{9,10}

In the present study, we have investigated by angle-resolved photoemission spectroscopy (ARPES), the formation of the two-dimensional electron gas on the nonreconstructed InAs(111)B(1×1) surface covered by Sn. An accumulation layer related feature appears in the photoemission spectrum above the conduction band minimum (CBM).

It exhibits a nonmonotonic intensity behavior with a maximum at 1 ML coverage.

The experiments were performed at beamline 41 at the national synchrotron radiation facility MAX-lab in Lund, Sweden. This beamline is equipped with a TGM monochromator, providing a photon energy range of 15 to 200 eV and has been describe elsewhere.¹¹ The experimental chamber is equipped with a VSW HA50 electron energy analyzer mounted on a goniometer for angular resolved measurements, a low-energy electron diffraction (LEED), an ion gun for sputter cleaning of samples, evaporation sources, a quartz crystal thickness monitor (QCM), and sample annealing possibilities.

The InAs(111)B samples were pieces of single crystal wafers (Wafer Technology Ltd.) of *n*-type with carrier concentration of $8.7 \times 10^{16} \text{ cm}^{-3}$. *In situ* cleaning comprised initial degassing, cycles of simultaneous argon-ion bombardment and annealing (500 eVAr⁺, 400 °C). The surface cleanliness and long-range order were checked in all cases using photoelectron spectroscopy and LEED.

Sn was deposited at room temperature (RT) from a thoroughly out-gassed source; the pressure in the chamber during evaporation was 2×10^{-9} Torr. The thickness of the deposited layer was measured with a QCM and was also estimated from photoemission intensities of In 4*d* and Sn 4*d* core levels, and from the shift of the secondary electron cutoff. The amount of deposited Sn is expressed in terms of monolayers (ML), where one monolayer is defined as the surface atomic density of the unreconstructed InAs(111)(1×1) plane ($8.14 \times 10^{14} \text{ cm}^{-2}$). After each deposition the surface was observed with LEED. In the initially sharp and low background (1×1) LEED pattern weak streaks appeared between the diffraction spots when approaching monolayer coverage, and at full monolayer additional spots could be seen. At higher coverage an increasing background was noticed around the weakened diffraction spots.

Angle resolved valence band spectra were measured along the $\bar{\Gamma}-\bar{K}$ azimuth using photon energies in the range 22–39 eV and an angular resolution $\sim 1^\circ$. The sample was oriented azimuthally using LEED. Core level spectra were measured in normal emission using 81 eV photons. The

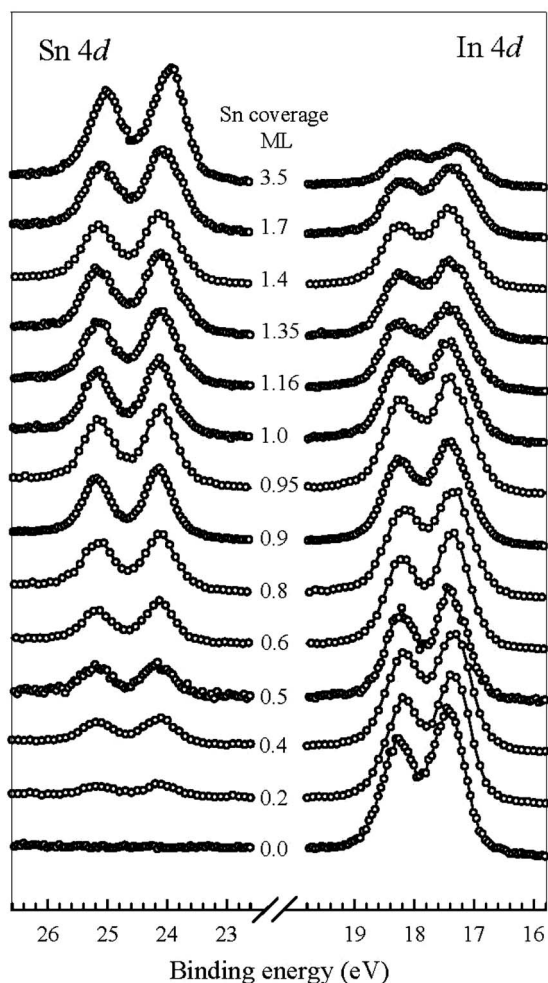


FIG. 1. ARPES spectra of InAs(111)(1×1)*B* Sn 4*d* and In 4*d* core level at different Sn coverage; $h\nu=81$ eV, $\theta=0^\circ$.

binding energies are given with respect to the Fermi level, measured from a clean Ta foil in electrical contact with the sample. The overall energy resolution was in the range 0.15–0.25 eV, estimated from the width of the Fermi level.

A set of In 4*d* and Sn 4*d* core levels recorded at different tin coverages are presented in Fig. 1. Sn deposition at RT does not induce any dramatic changes in the shape of these core levels. From the raw data one observes a broadening of the In 4*d* core level. A numerical fit quantifies this broadening from 0.42 eV on the clean to 0.57 eV on the tin covered surface at 1 ML using a two-component analysis.⁶

A plot of the Sn4*d*/In4*d* total integrated intensity ratio versus tin coverage in Fig. 2(a) displays a linear increase up to around 1 ML, where a small but clear change in the slope occurs. Such a behavior indicates that the first monolayer grows smoothly. The changes in Fermi level position and work function are presented in Fig. 2(b). The Fermi level movement is derived from the shift of the bulk component of the In 4*d* component extracted from the numerical fitting procedure. Since there are no clear features in the In 4*d* spectra, the fitting procedure can give somewhat imprecise results. However, fitting with either three or two components shows the same tendency for the Fermi level pinning.

On the clean surface the Fermi level is pinned very close

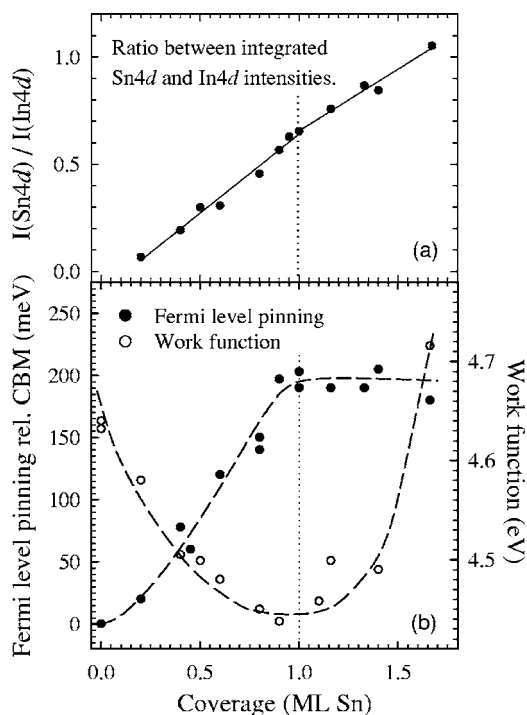


FIG. 2. (a) The Sn 4*d*/In4*d* total peak intensities ratio as a function of Sn coverage. (b) Fermi level pinning InAs(111)(1×1)*B* as a function of Sn coverage and Sn-induced work function changes.

to, but below, the conduction band minimum (CBM),⁶ hence no accumulation layer is generated. Adsorption of Sn causes a gradual shift of the Fermi level up into the conduction band, where it remains stable to ~1.6 ML. At higher coverages the Fermi level shifts back to the initial position below CBM (not shown). Sn adsorption thus induces a downward band bending, such that the Fermi level is found at ~0.2 eV above the CBM at ~1 ML coverage. This behavior differs qualitatively from the situation of, e.g., Cs/InAs(110), in which case the maximum Fermi level shift above CBM is induced by a very small fraction (0.01) of one Cs monolayer. In the present case the observations thus indicate that the pinning situation is stabilized by the adlayer itself rather than by donor type surface defects.

The Sn-induced work function changes were determined from the shift of the cutoff of secondary electrons. As shown in Fig. 2(b) the work function is gradually reduced, with a minimum when the first Sn layer is completed. At higher coverage, the work function increases. The work function changes are clearly linked with the band bending.

Valence band spectra recorded with 27 eV photons for increasing amounts of Sn at RT are presented in Fig. 3; the tin coverage is indicated in the figure. The bottom spectrum was recorded from the clean surface, and it corresponds to previously published data from the same surface.⁷ The shape and interpretations of peaks S_1 , and S_2 follows that of Ref. 7. At low coverage, the effect of Sn is primarily observed at S_1 , which originates from fully occupied As-dangling bonds. At normal emission, this surface state is already quenched at 0.4 ML. At 5 eV binding energy the S_2 peak, assigned to back-bond states, is practically unchanged. Two bulk structures

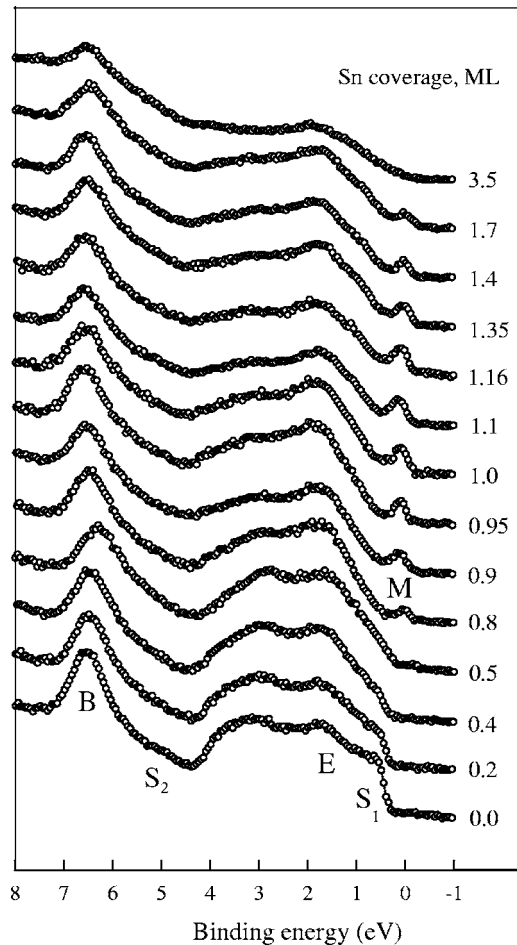


FIG. 3. ARPES spectra of InAs(111)(1x1)B valence band at different Sn coverage; $h\nu=27$ eV, $\theta=0^\circ$. Labeled peaks are described in the text.

around 2 eV (marked E) and 6.3 eV (marked B) are also noticed. Their intensities decrease slowly with increasing Sn coverage. The first sign of emission from a new Sn-induced state ("M") at the Fermi level appears between 0.4 and 0.5 ML coverage, and augments steadily up to the completion of the first Sn monolayer. With further Sn adsorption the intensity decreases, and vanishes completely at 3.5 ML.

The excitation energy dependence of peak M in the range 22–39 eV is shown in Fig. 4(a). This series of spectra were collected at the Sn thickness of 0.8 ML, which is slightly below the intensity maximum of M. Within the limits of experimental resolution, no dispersion was observed along the direction normal to the surface in the measured photon energy range. The maximum cross section is observed at the photon energy of ~ 27 eV. It is significant to note that this energy does not match cross section maxima¹ (around 20 eV and 45 eV) for the intrinsic electron gas state on InAs(111)A. The resonant behavior of the cross section does, however, show that the excitation involves an interband transition, just like on the(111)A surface. This is a rather different scenario than that reported for, e.g., the Pb/InAs(100) system,¹² in which case the increased intensity of the charge accumulation peak after Pb adsorption was ascribed to spatial redistribution of the accumulation layer. In the same way the present

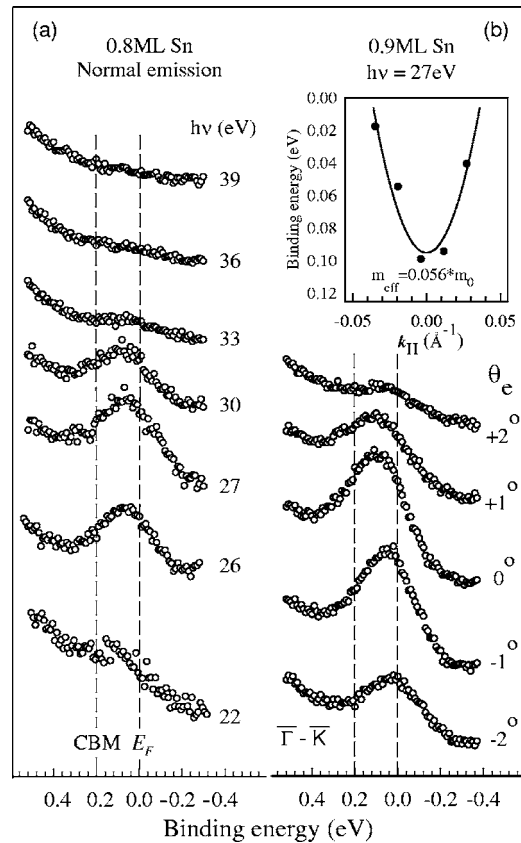


FIG. 4. (a) ARPES spectra of the *M* feature after deposition of 0.8 ML Sn at RT, for different photon energies; $\theta=0^\circ$. (b) ARPES spectra of the *M* feature for different emission angles along $\bar{\Gamma}-\bar{K}$ (0.9 Sn ML); $h\nu=27$ eV. A free-electron parabola fitted to the experimental dispersion along $\bar{\Gamma}-\bar{K}$ of the *M* feature is presented in the insert.

observations also differ from those on the Fe/InAs(110) system,¹³ in which case the vanishing conduction band state emission at photon energies above 25 eV was ascribed to the mean free path reduction with increasing electron energy.

The conduction band emission is observed only within a range of approximately $\pm 2^\circ$ around the surface normal as shown in Fig. 4(b). The spectra were measured from the surface covered with 0.9 ML Sn along the $\bar{\Gamma}-\bar{K}$ direction of the SBZ. The emission is confined to a narrow angular range with a maximum around the $\bar{\Gamma}$ point, very similar to what has been reported for clean as well as adsorbate-perturbed InAs surfaces.^{1,14}

In the inset of Fig. 4(b) we present a fit of the dispersion along $\bar{\Gamma}-\bar{K}$ to a nearly free electron parabola that confirms the free electron character of the electrons in the confined layer. The value for the effective mass extracted from this is $0.056 m_0$, which is in good agreement with what was found for the InAs(110)-Cs surface.³

We note that while the dispersion of peak *M* is symmetric around $\bar{\Gamma}$, the intensity distribution appears to lack the symmetry. This is totally unexpected, as the substrate Brillouin zone (surface as well as bulk) is perfectly symmetric along the two directions. Considering that the variation occurs over

a very small angular range, we hold it unlikely that the observed asymmetry is an experimental artifact (e.g., due to some kind of misalignment or presence of external fields). The origin of this asymmetry remains unexplained. A similar asymmetry, with higher intensity in the direction toward the incident photon beam was also observed along the $\bar{\Gamma}-\bar{M}$ azimuth, but in this case one might ascribe it to the non-equivalence between the \bar{M} and \bar{M}' azimuths.

As already stated, our observations show that the M structure originates from a 2DEG, but at the same time some of the spectroscopic properties are distinctly different from previous reports of similar structures on other InAs surfaces. The fact that the structure is seen only in a narrow angular range around the surface normal, and that it appears only when the band bending shifts the conduction band minimum below the Fermi level, supports the idea that it reflects occupied conduction band states in InAs. It is in fact the narrow range in k space of the CBM that renders for InAs (and InSb) the unusual location of the charge neutrality level above CBM (Ref. 15). The large band dispersion at CBM implies an extremely low density of states, which is the prerequisite for the filling of these states by minute amounts of charge. Previous photoemission observations of charge accumulation have been possible to ascribe to donor-type surface defects. In this respect the present results deviate from earlier reports, as the charge accumulation emission is seen to develop gradually in the present case, up to monolayer coverage. The obvious question is then what makes the InAs(111) B surface unique (or unusual) in this context. We tentatively associate this with another unusual property of this surface, namely its stability in a nonreconstructed state. According to a theoretical treatment of the InAs(111) $B(1 \times 1)$ surface, its electrostatic stability can be explained by the formation of a surface dipole, which can occur as a result of an asymmetric average potential around the anion-cation double planes.⁵ This structural and electronic stability hinders the formation of a 2DEG from donor-type surface defects (which ought to be as common on this surface as on other InAs surfaces). However, with the adsorption of Sn there is an alternative source of charge, namely the Sn atoms themselves. Since the surface is initially As terminated, each adsorbed Sn atom takes the position of an In atom in an “extended lattice structure.” It is then reasonable to expect the Sn atoms in the first adsorbed layer to act as donors. The gradual development of the CBM emission structure can thus be considered to be a natural consequence of increasing n -type doping. Another

obvious consequence of the appearance of surface donors is the gradual reduction of the work function. The work function is of course a complex integrated quantity, which may include, e.g., effects of possible depolarization of the initial electronic distribution.⁷ However, such depolarization should lead to an increased work function, so we conclude that the final changes of the surface dipole are dominated by the appearance of a positive charge in the outermost surface plane.

The scenario outlined above is also consistent with the upward band bending and increase of work function for Sn coverage beyond one monolayer. In this case the Sn donors occupying the first surface plane should be affected by Sn neighbors in the outer plane, and their role as substitutes of In in an InAs lattice (i.e., their role as donors) should become less favorable.

We have stressed that the resonant behavior of the CBM emission reveals that the excitation process is essentially a bulk interband transition. From this point of view we should expect to observe excitation maxima at the same photon energies as for the clean InAs(111) A surface. The fact that this is not the case is tentatively ascribed to a modified inner potential in the “delta-doped” region.

The anomalous broadening of the In $4d$ bulk peak, from 0.42 eV on the clean surface to 0.57 eV at 1 ML Sn coverage may indicate a localization of the accumulation layer close to the surface. With an uncertainty of +50 meV in these values we estimate the additional broadening to be 0.2–0.4 eV, keeping in mind that different contributions add quadratically. At low submonolayer coverages this could be due to inhomogeneous band bending over the surface. This is, however, not the case for the monolayer-covered surface. Instead, the broadening may be due to a rapid variation of the band bending in the z direction.

To conclude, we have studied the formation of an accumulation layer at the InAs(111) $B(1 \times 1)$ surface upon Sn adsorption. A structure related to a two-dimensional electron gas appears in the photoemission spectrum close to the Fermi level, above the conduction band minimum at monolayer Sn coverage. We ascribe the development of this charge accumulation layer to the n -doping property of Sn when it substitutes In in the InAs lattice.

We are grateful for the financial support from the Swedish Research Council, the Göran Gustafsson Foundation. We also acknowledge the support from the Swedish synchrotron radiation source MAX-lab, Lund.

*Corresponding author: ksl@imit.kth.se

¹L. Ö. Olsson, C. B. M. Andersson, M. C. Håkansson, J. Kanski, L. Ilver, and U. O. Karlsson, *Phys. Rev. Lett.* **76**, 3626 (1996).

²P. De Padova, C. Quaresima, P. Perfetti, R. Lariciprete, R. Brochier, C. Richter, V. Ilakovac, P. Bencok, C. Teodorescu, V. Y. Aristov, R. L. Johnson, and K. Hricovini, *Surf. Sci.* **482–485**, 587 (2001).

³V. Yu. Aristov, G. Le Lay, V. M. Zhilin, G. Indlekofer, C. Grupp,

A. Taleb-Ibrahimi, and P. Soukiassian, *Phys. Rev. B* **60**, 7752 (1999).

⁴C. B. M. Andersson, U. O. Karlsson, M. C. Håkansson, L. Ö. Olsson, L. Ilver, P.-O. Nilsson, J. Kanski, and P. E. S. Persson, *Phys. Rev. B* **54**, 1833 (1996).

⁵S. Mankefors, P.-O. Nilsson, and J. Kanski, *Surf. Sci.* **443**, L1049 (1999).

⁶K. Szamota-Leandersson, M. Göthelid, O. Tjernberg, and U. O.

- Karlsson, *Appl. Surf. Sci.* **212–213**, 589 (2003).
- ⁷C. B. M. Andersson, U. O. Karlsson, M. C. Håkansson, L. Ö. Olsson, L. Ilver, J. Kanski, P.-O. Nilson, and P. E. S. Persson, *Surf. Sci.* **307–309**, 885 (1994).
- ⁸W. T. Yuen, W. K. Liu, S. N. Holmes, and R. A. Stradling, *Semicond. Sci. Technol.* **4**, 819 (1989).
- ⁹I. Hernandez-Calderon, H. Höchst, A. Mazur, and J. Pollmann, *J. Vac. Sci. Technol. A* **5**, 2042 (1987).
- ¹⁰P. Fantini, S. Gardonio, P. Barbieri, U. Del Pennino, C. Mariani, M. G. Betti, E. Magnano, M. Pivetta, and M. Sancrotti, *Surf. Sci.* **463**, 174 (2000).
- ¹¹U. O. Karlsson, J. N. Andersen, K. Hansen, and R. Nyholm, *Nucl. Instrum. Methods Phys. Res. A* **282**, 553 (1989).
- ¹²J. M. Layet, M. Carrera, H. J. Kim, R. L. Johnson, R. Belkhou, V. Zhilin, V. Yu. Aristov, and G. Le Lay, *Surf. Sci.* **402/404**, 724 (1998).
- ¹³M. Morgenstern, M. Getzlaff, D. Haude, R. Wiesendanger, and R. L. Johnson, *Phys. Rev. B* **61**, 13805 (2000).
- ¹⁴V. Yu. Aristov, T. M. Grehk, V. M. Zhilin, A. Taleb-Ibrahimi, G. Indlekofer, Z. Hurych, G. Le Lay, and P. Soukiassian, *Appl. Surf. Sci.* **104/105**, 73 (1996).
- ¹⁵J. Tersoff, *Phys. Rev. B* **32**, 6968 (1985).